Supporting Information

Heteroatom-bridged ortho-Biferrocenes: Stereoselective Synthesis, Structural Features and Electrochemical Properties

*Jiawei Chen,[a] Alain C. Tagne Kuate,[a,b] Roger A. Lalancette,[a] and Frieder Jäkle[a]**

[a] Department of Chemistry, Rutgers University-Newark, 73 Warren Street, Newark, NJ 07102, USA.

[b]Department of Chemistry, Faculty of Sciences, University of Dschang, P.O. Box 67, Dschang, Cameroon

* To whom correspondence should be addressed. E-mail: fjaekle@rutgers.edu

X-RAY CRYSTALLOGRAPHY STUDIES

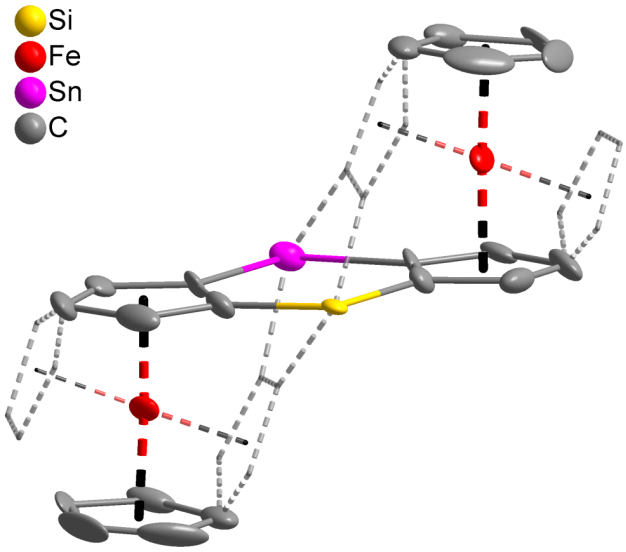

Figure S1. During the refinement of the structure for **2-SnSi**, another set of Q peaks, representing an alternative orientation of the disordered diferrocene unit, could be found (dashed line, all hydrogens and methyl carbons are omitted for clarity). However, the disorder was not modeled. Constraints such as ISOR and DELU were used to compensate this issue.

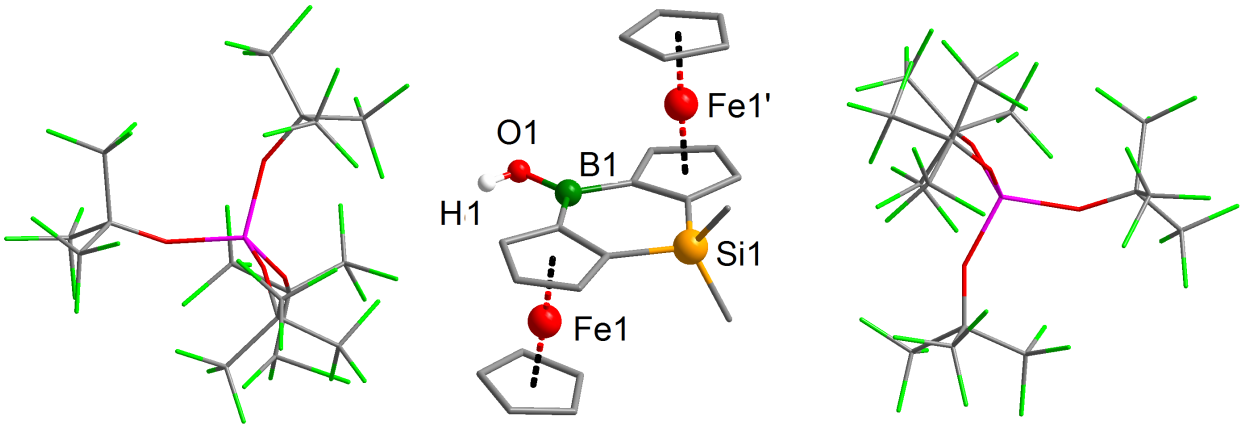

Figure S2. Plot of the single crystal X-ray structure of the doubly oxidized, hydrolyzed species **3-BSi** derived from **2-BSi** (hydrogen atoms omitted except for B-OH). The structure solution suffered from disorder issues and is only presented to demonstrate connectivity.

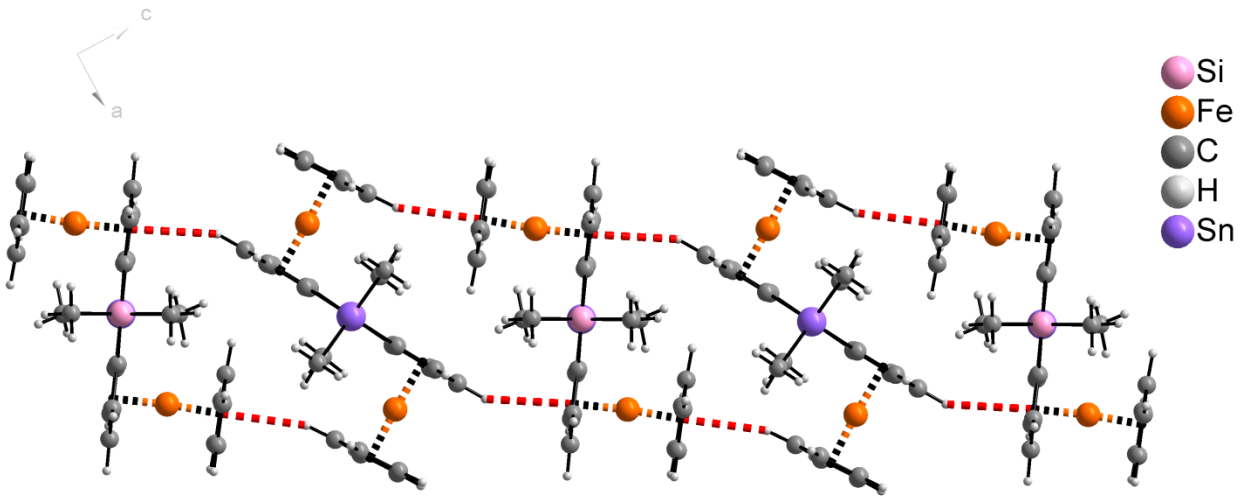

Figure S3. Plot illustrating the supramolecular structure of **2-SnSi**

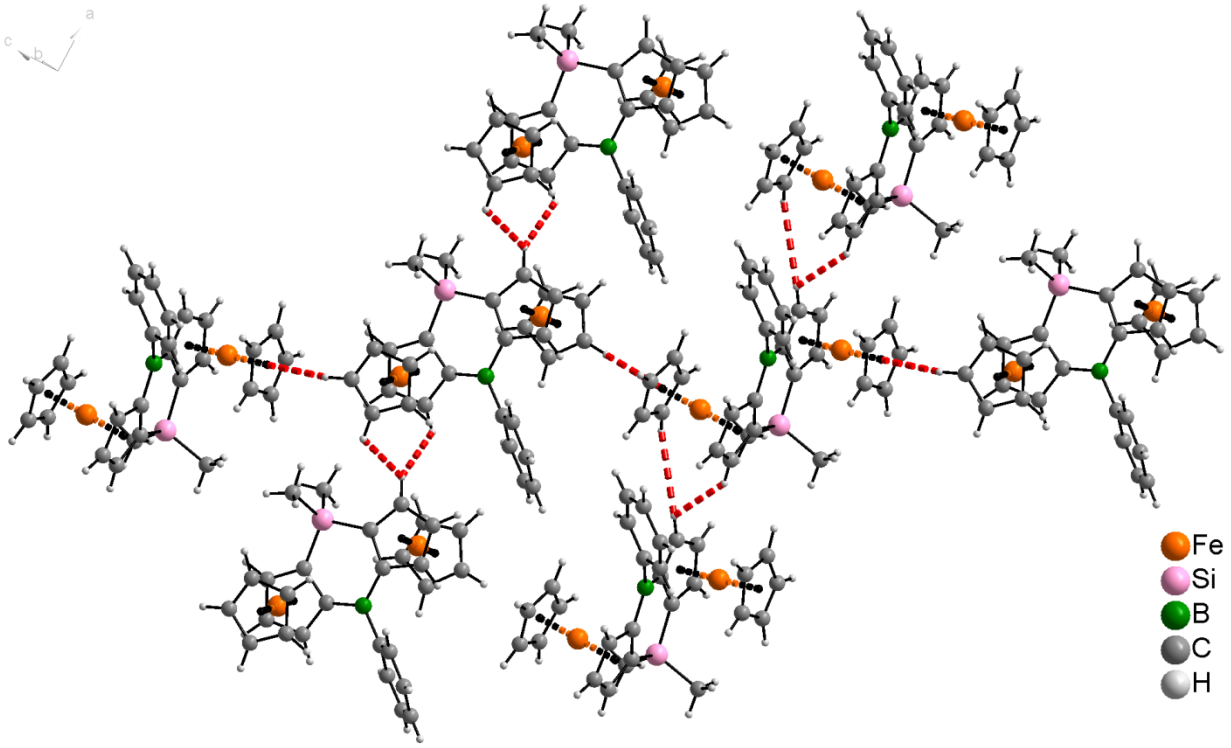

Figure S4. Plot illustrating the supramolecular structure of **2-BSi**

Table S1. Crystal data and structure refinement details for (p*R*,p*R*,S_S,S_S)-**1-Sn**, (p*R*, p*R*)-**2-SnSi**, (p*R*, p*R*)-**2-SnP**, and (p*R*, p*R*)-**2-BSi**.

Compound	(p*R*,p*R*,S_S,S_S)-**1-Sn**	(p*R*, p*R*)-**2-SnSi**	(p*R*, p*R*)-**2-SnP**	(p*R*, p*R*)-**2-BSi**
CSD Entry	**1470561**	**1470562**	**1470563**	**1470564**
empirical formula	$C_{36}H_{36}Fe_2O_2S_2Sn$	$C_{20}H_{28}Fe_2SiSn$	$C_{26}H_{34}BFe_2PSn$	$C_{28}H_{27}BFe_2Si$
MW	795.16	574.94	618.70	514.10
T, K	100(2)	100(2)	100(2)	100(2)
wavelength, Å	1.54178	1.54178	1.54178	1.54178
crystal system	Triclinic	Monoclinic	Orthorhombic	Monoclinic
space group	*P*1	*C*2	$P2_12_12_1$	$P2_1$
a, Å	7.6712 (2)	13.2479 (4)	12.1285 (2)	9.0969 (2)
b, Å	10.7861 (2)	13.5201 (4)	13.3506 (2)	7.3330 (1)
c, Å	10.8306 (2)	13.9401 (6)	15.4421 (2)	17.4165 (3)
α, deg	64.332 (1)	90	90	90
β, deg	83.343 (1)	117.891 (2)	90	93.957 (1)
γ, deg	77.207 (1)	90	90	90
V, Å^3	787.46 (3)	2206.81 (13)	2500.43 (6)	1159.04 (5)
Z	1	4	4	2
ρ_{calc}, g cm^{-3}	1.677	1.730	1.644	1.473
μ (Cu Kα), mm^{-1}	15.04	19.89	17.74	10.62
crystal size, mm	0.41×0.29×0.22	0.39×0.20×0.13	0.30×0.23×0.12	0.39×0.26×0.06
θ range, deg	4.5-73.7	3.6-70.7	4.4-71.3	2.5-70.4
limiting indices	$-9\le h\le 9$	$-16\le h\le 15$	$-10\le h\le 14$	$-10\le h\le 10$
	$-11\le k\le 13$	$-16\le k\le 16$	$-15\le k\le 16$	$-8\le k\le 7$
	$-12\le l\le 12$	$-16\le l\le 16$	$-18\le l\le 17$	$-19\le l\le 20$
reflns collected	7944	9272	24052	9201
independent reflns	3836 [*R*(int) = 0.024]	3538 [*R*(int) = 0.036]	4398 [*R*(int) = 0.035]	3271 [*R*(int) = 0.035]
absorption correction	Numerical	Numerical	Numerical	Numerical
data/restraints/para's	3836 / 3 / 392	3538 / 8 / 261	4398 / 0 / 286	3271 / 1 / 291
goodness-of-fit on F^2	1.04	1.17	1.05	1.01
final *R* indices	*R*1 = 0.025	*R*1 = 0.050	*R*1 = 0.032	*R*1 = 0.025
[I >2σ(I)] [a]	w*R*2 = 0.060	w*R*2 = 0.114	w*R*2 = 0.044	w*R*2 = 0.062
R indices (all data) [a]	*R*1 = 0.022	*R*1 = 0.052	*R*1 = 0.019	*R*1 = 0.026
	w*R*2 = 0.060	w*R*2 = 0.117	w*R*2 = 0.044	w*R*2 = 0.062
peak$_{max}$/hole$_{min}$ (e Å^{-3})	0.94 / –0.49	1.02 / –1.12	0.52 / –0.32	0.38 / –0.22
Flack parameter	0.018(3)	0.114(17)	0.008(4)	0.007(3)

[a] $R1 = \Sigma||F_o|-|F_c||/\Sigma|F_o|$; $wR2 = [\Sigma[w(F_o^2-F_c^2)^2]/\Sigma[w(F_o^2)^2]]^{1/2}$

UV-VIS SPECTRAL ANALYSES

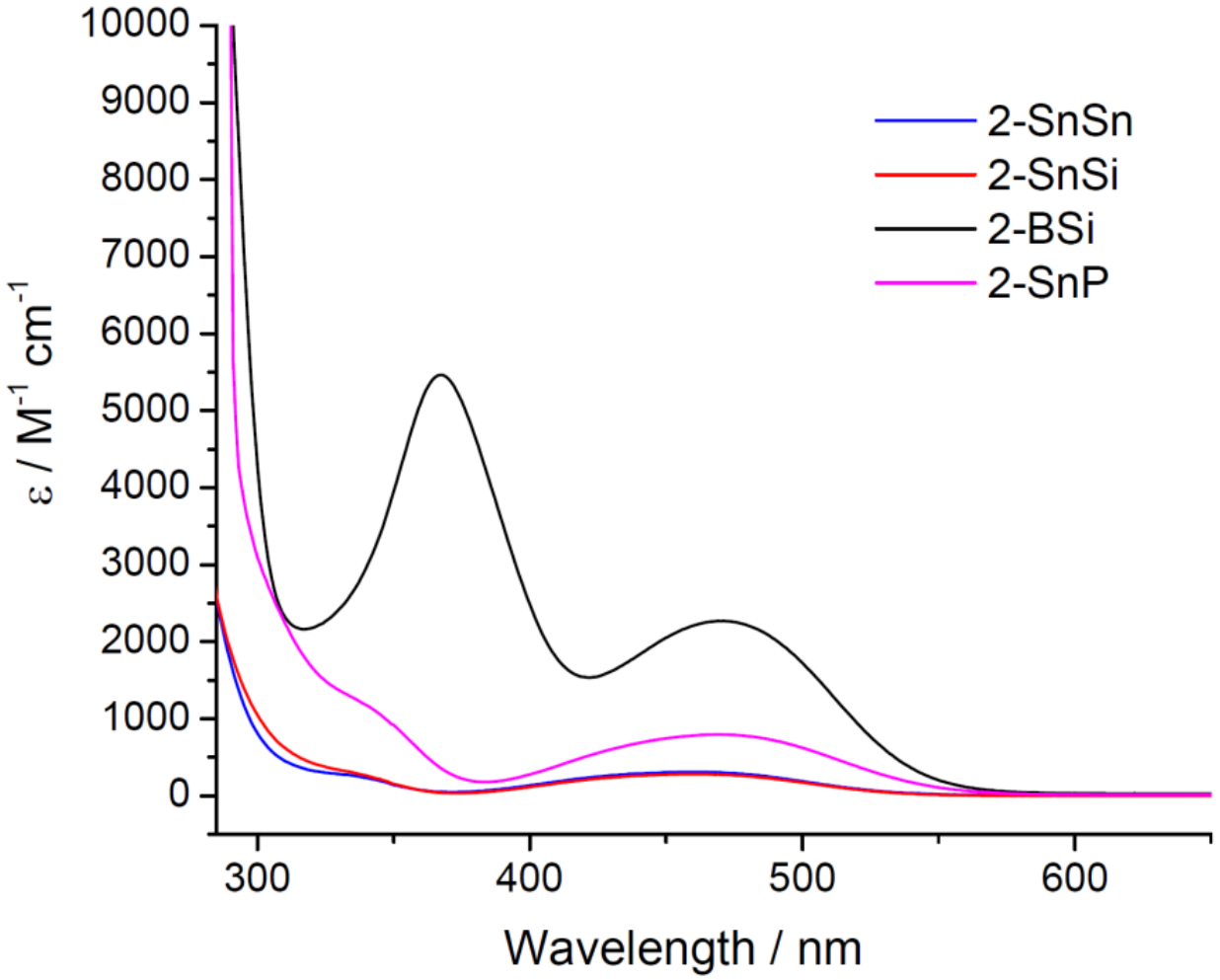

Figure S5. UV/Vis absorption spectra of **2-SnSn** (blue), **2-SnSi** (red), and **2-SnP** (purple), and **2-BSi** (black) in CH_2Cl_2

CHIRAL HPLC ANALYSES

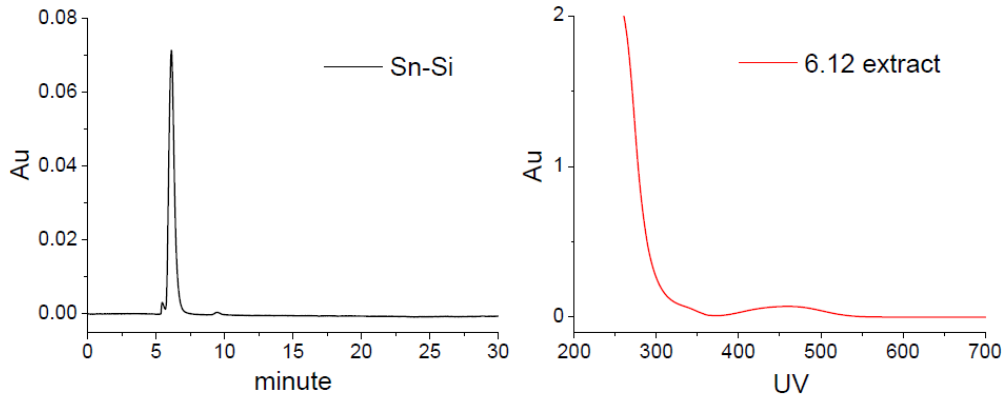

Figure S6. Chiral HPLC trace and the corresponding UV-Vis spectrum of **2-SnSi** using hexanes/THF (98:2) as eluent

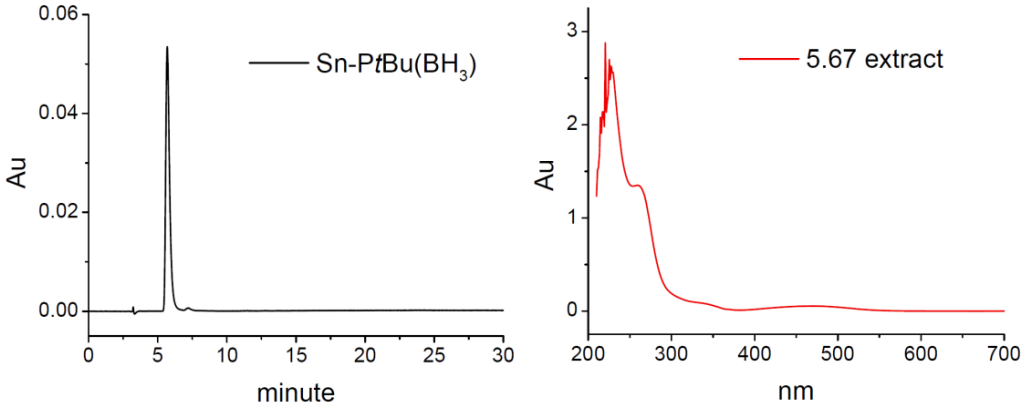

Figure S7. Chiral HPLC trace and the corresponding UV-Vis spectrum of **2-SnP** using hexanes/THF (90:10) as eluent

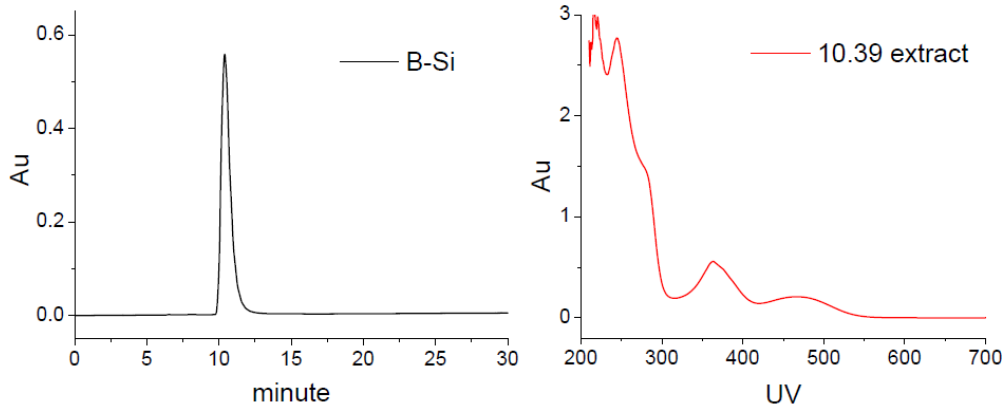

Figure S8. Chiral HPLC trace and the corresponding UV-Vis spectrum of **2-BSi** using hexanes/THF (98:2) as eluent

COPIES OF NMR SPECTRA

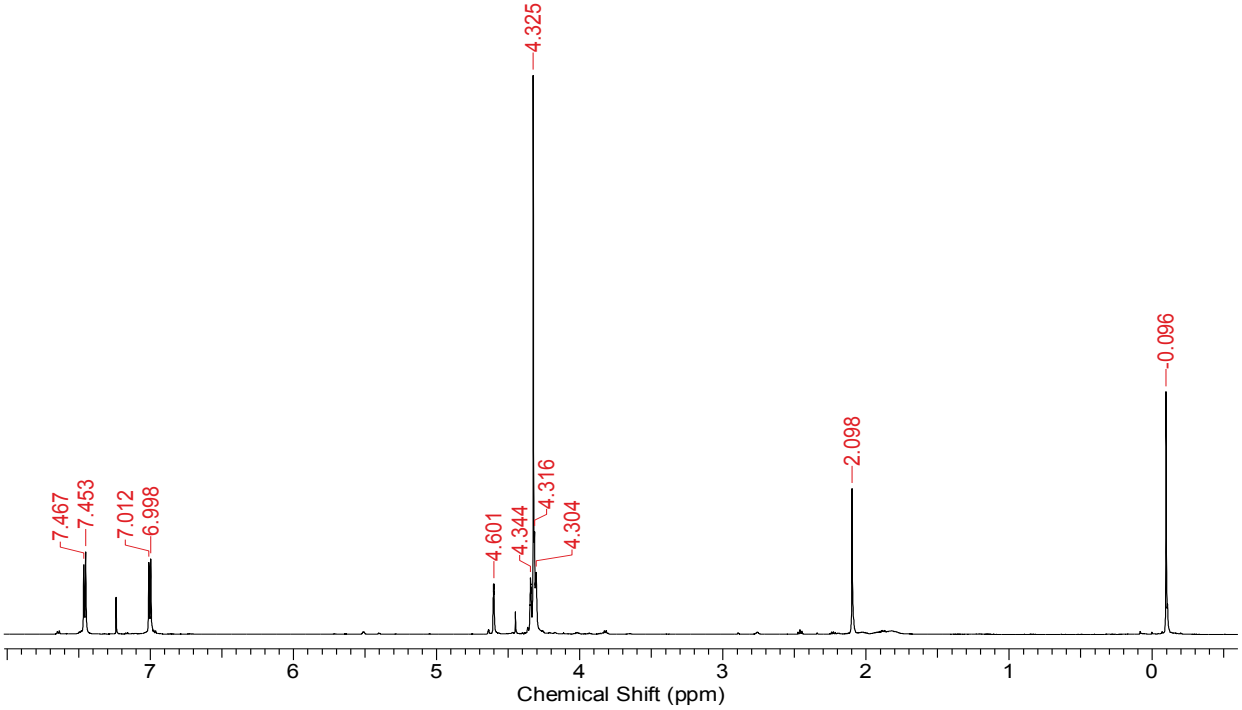

Figure S9. ^{1}H NMR spectrum of **1-Si'** in $CDCl_3$

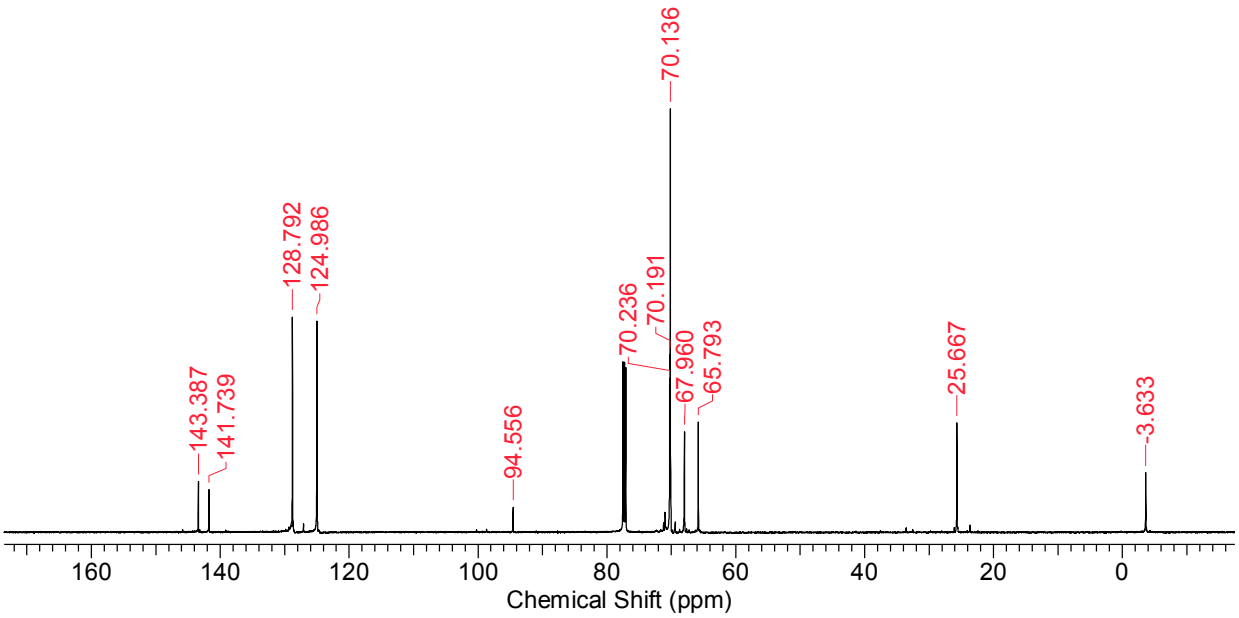

Figure S10. ^{13}C NMR spectrum of **1-Si'** in $CDCl_3$.

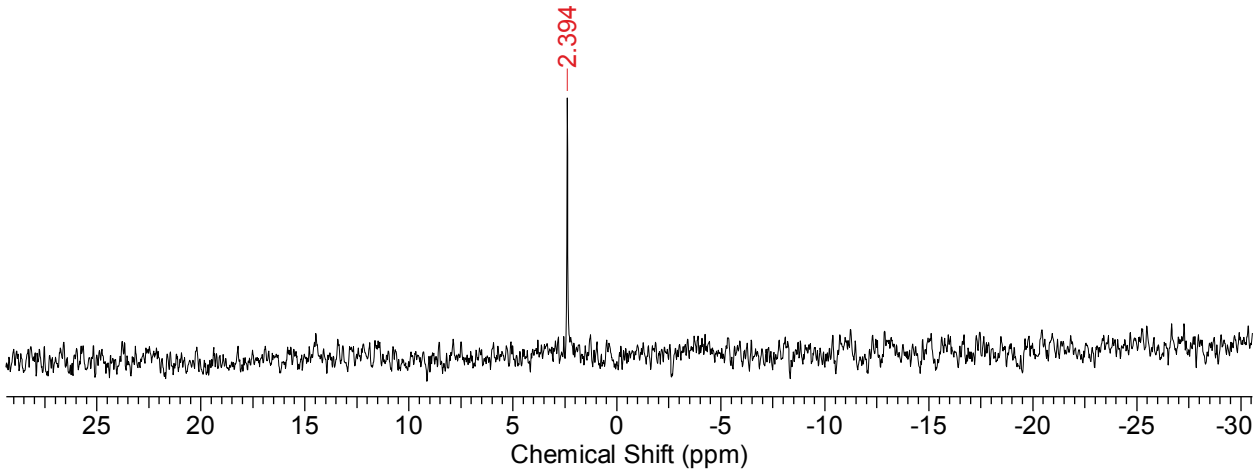

Figure S11. ^{29}Si NMR spectrum of **1-Si'** in $CDCl_3$.

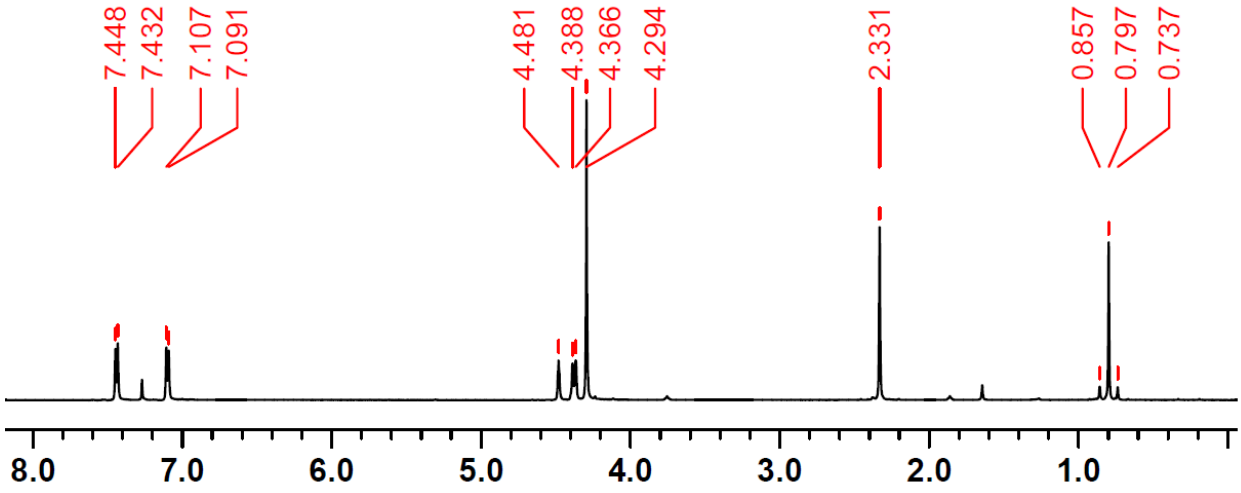

Figure S12. ^{1}H NMR spectrum of **1-Sn** in $CDCl_3$

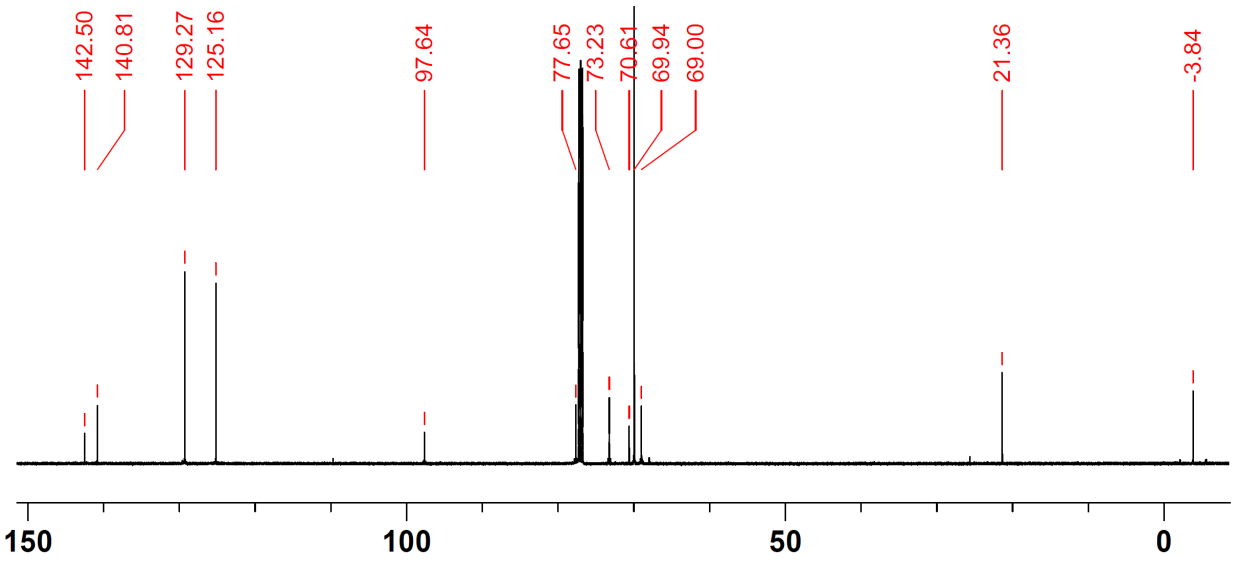

Figure S13. ^{13}C NMR spectrum of **1-Sn** in $CDCl_3$.

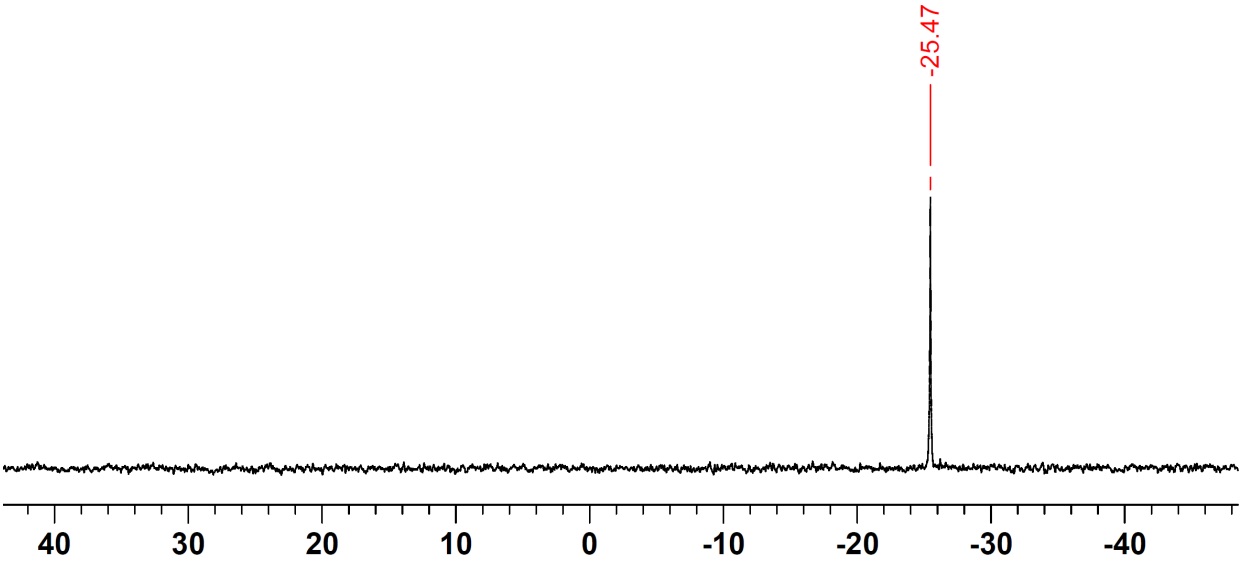

Figure S14. ^{119}Sn NMR spectrum of **1-Sn** in $CDCl_3$.

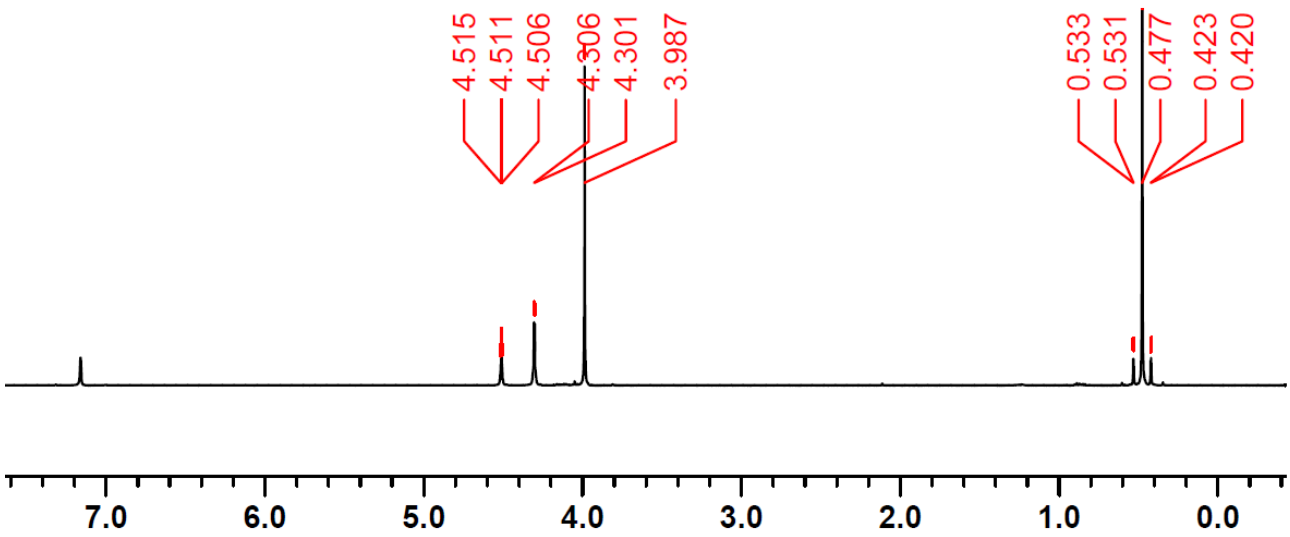

Figure S15. ^{1}H NMR spectrum of **2-SnSn** in C_6D_6

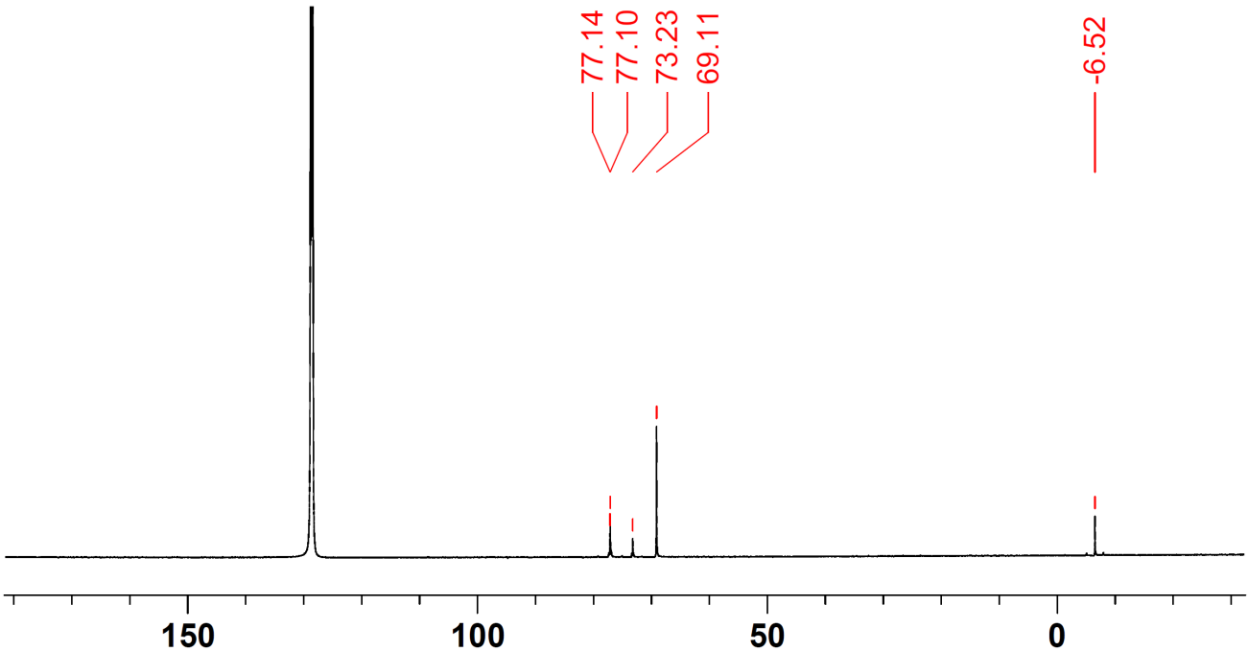

Figure S16. ^{13}C NMR spectrum of **2-SnSn** in C_6D_6

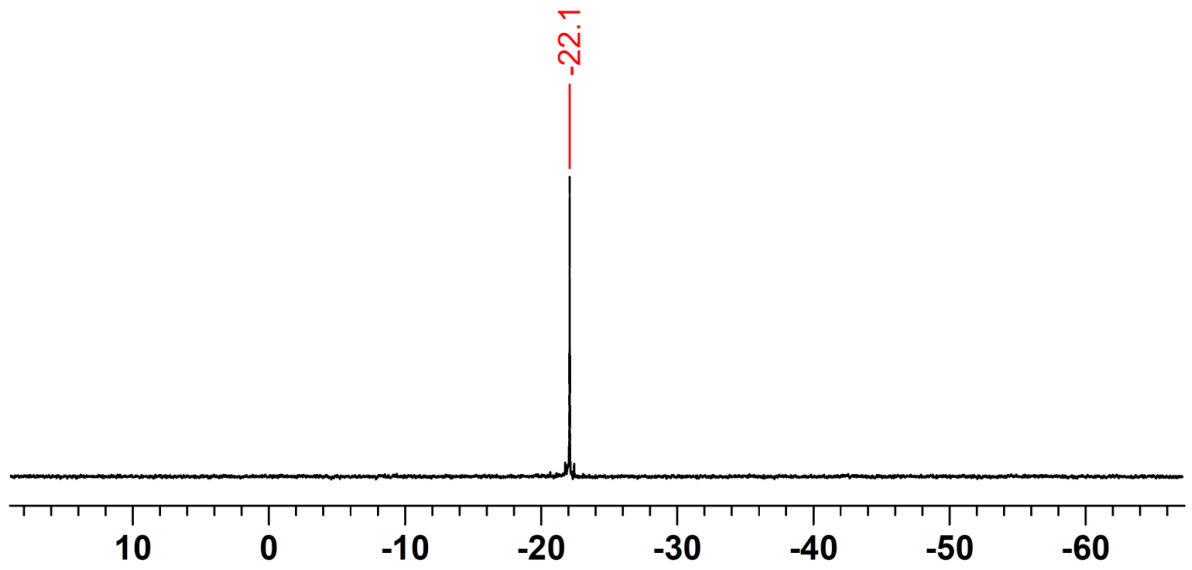

Figure S17. ^{119}Sn NMR spectrum of **2-SnSn** in C_6D_6

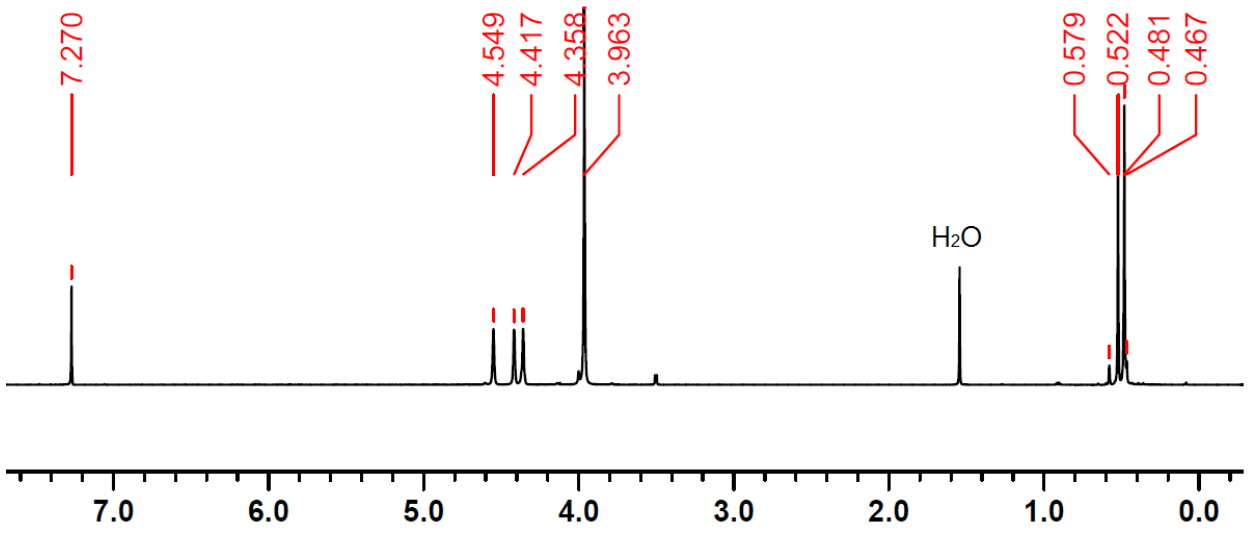

Figure S18. ^{1}H NMR spectrum of **2-SnSi** in $CDCl_3$

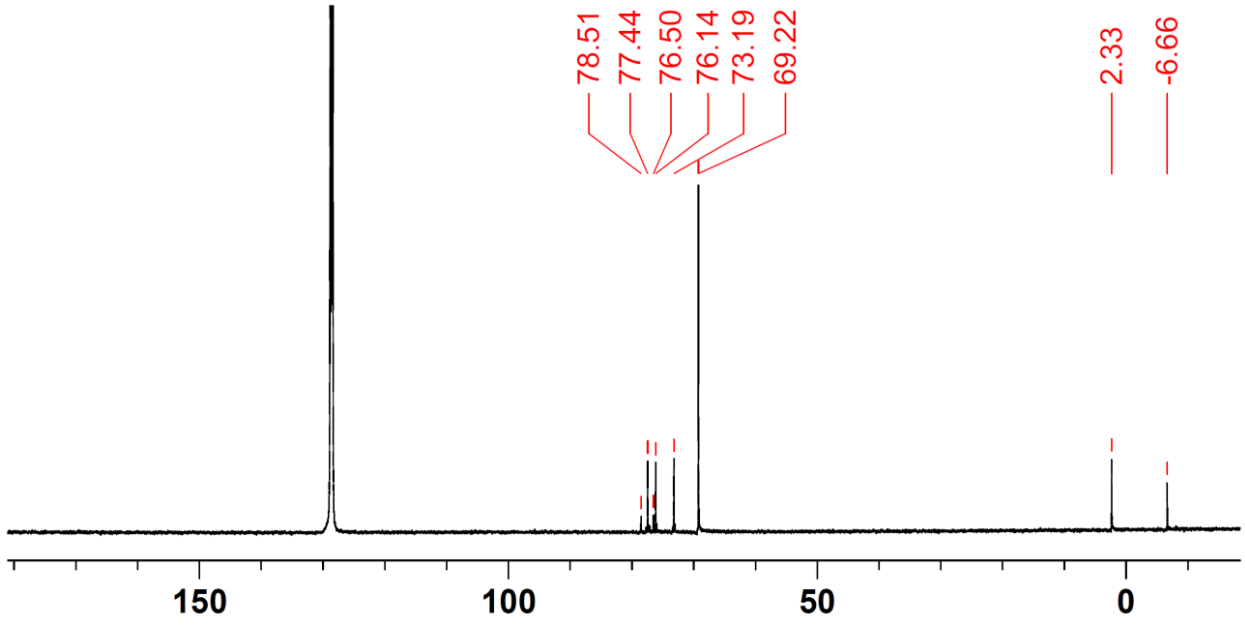

Figure S19. ^{13}C NMR spectrum of **2-SnSi** in C_6D_6

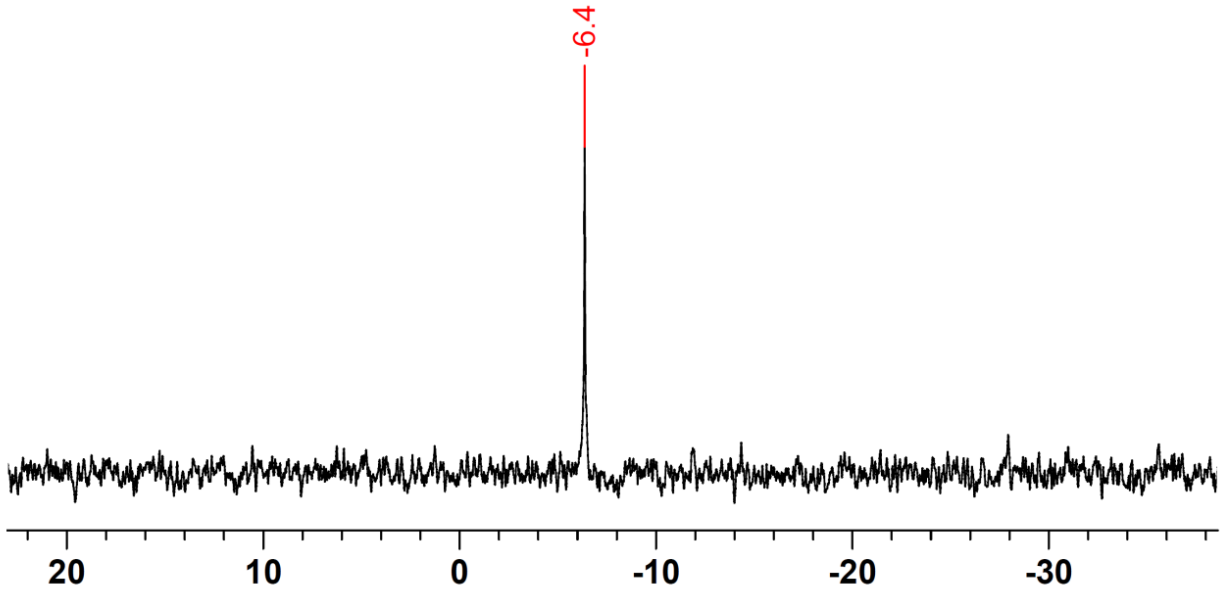

Figure S20. ^{29}Si NMR spectrum of **2-SnSi** in C_6D_6

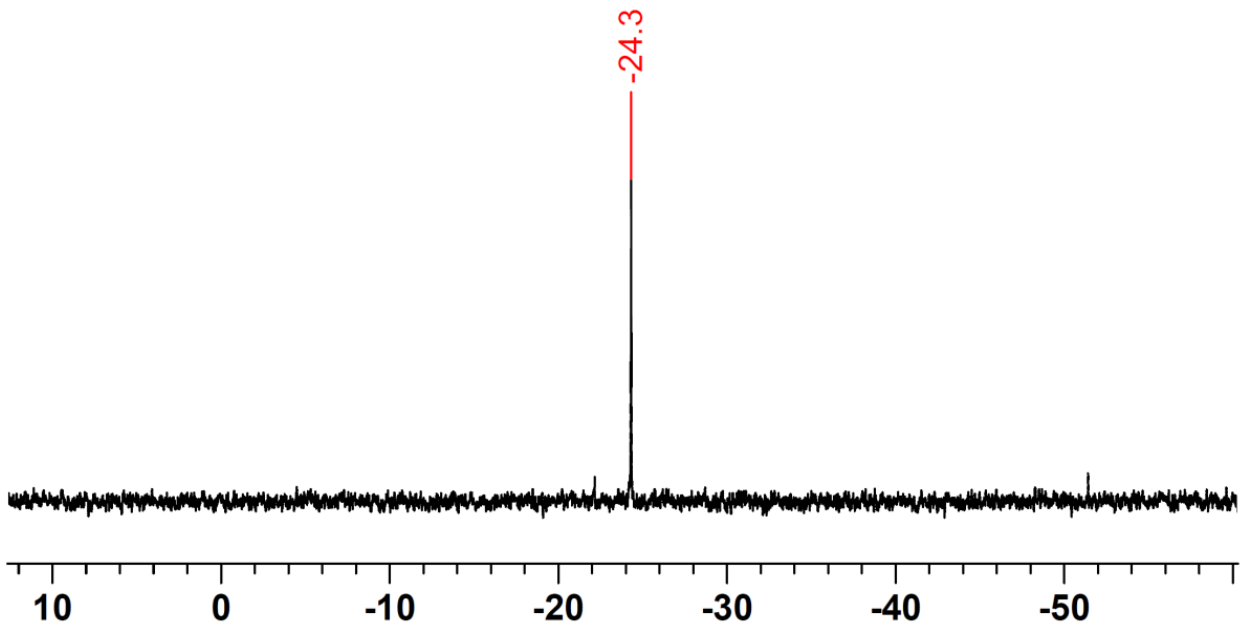

Figure S21. ^{119}Sn NMR spectrum of **2-SnSi** in C_6D_6

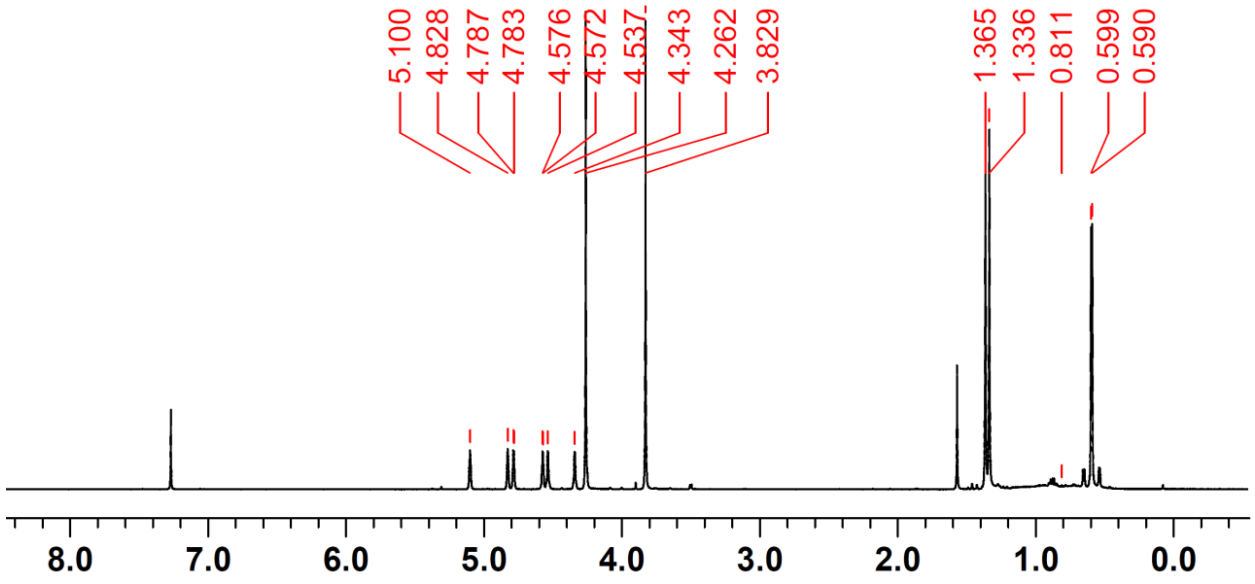

Figure S22. ^{1}H NMR spectrum of **2-SnP** in $CDCl_3$

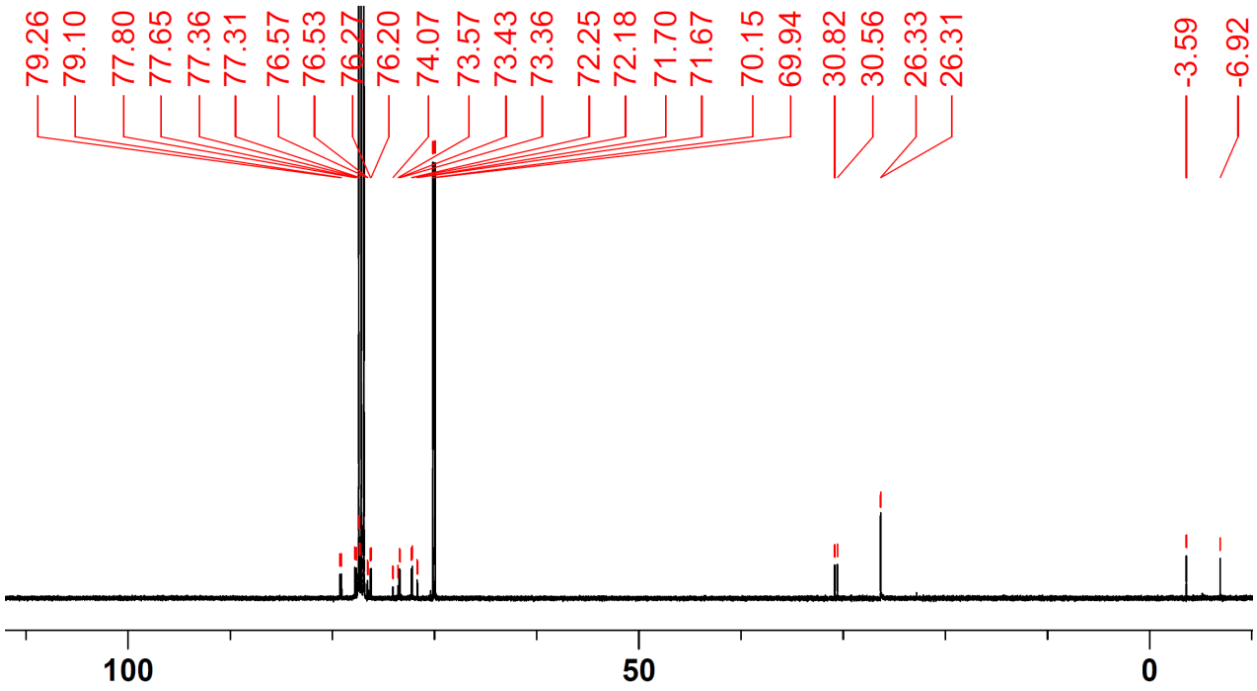

Figure S23. ^{13}C NMR spectrum of **2-SnP** in $CDCl_3$

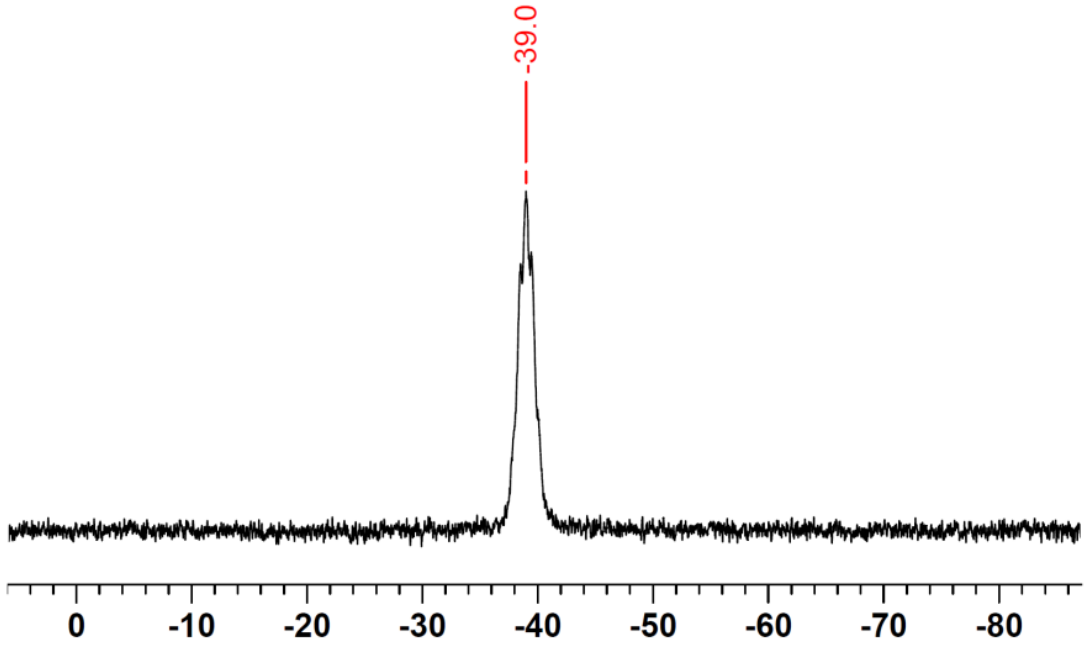

Figure S24. ^{11}B NMR spectrum of **2-SnP** in $CDCl_3$

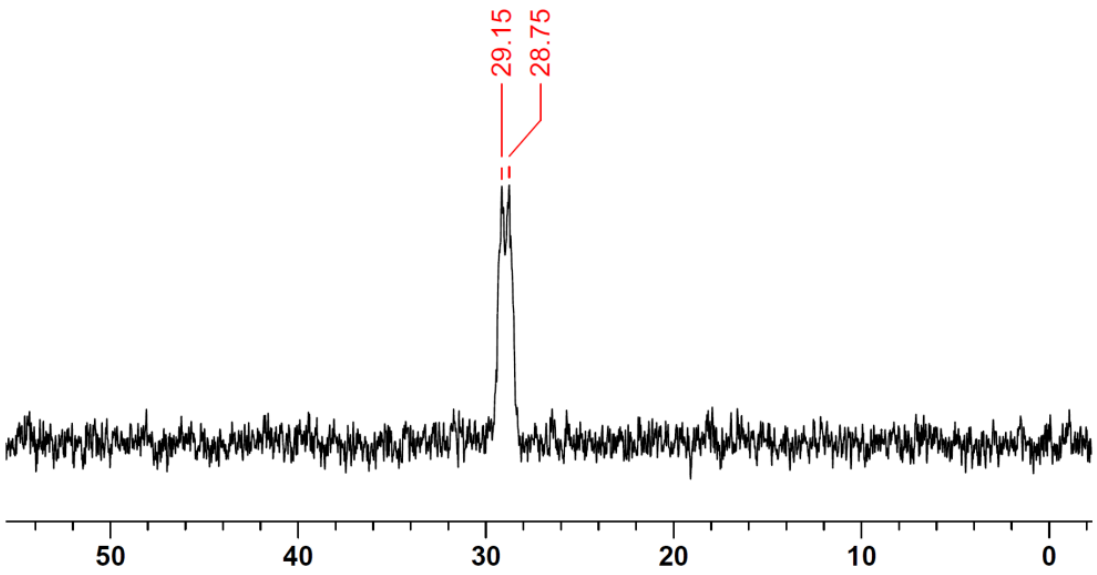

Figure S25. ^{31}P NMR spectrum of **2-SnP** in $CDCl_3$

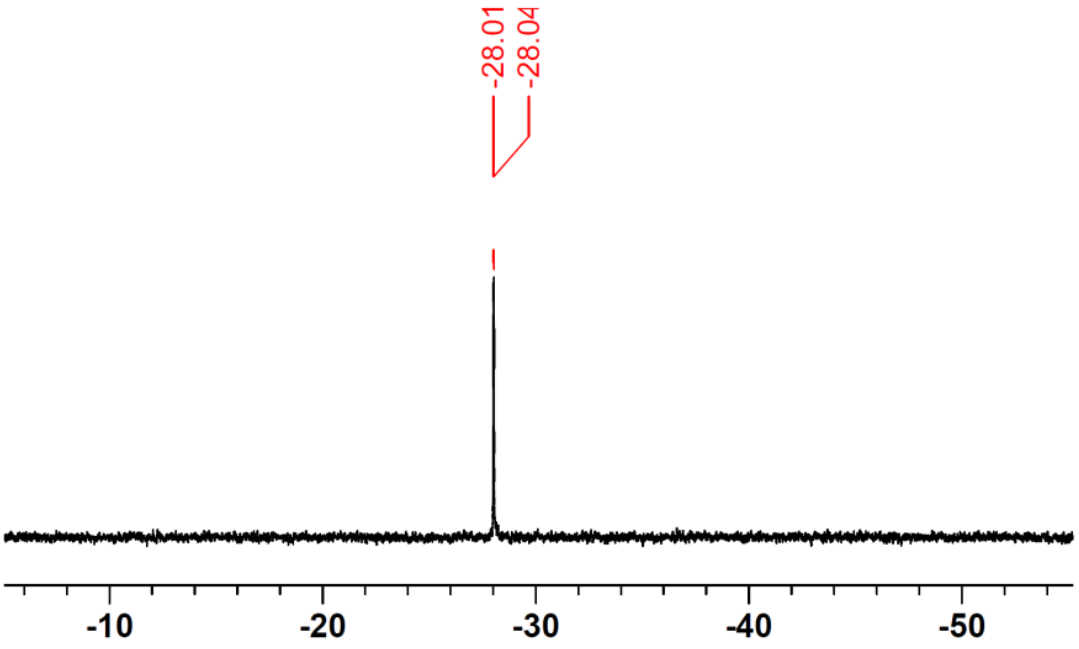

Figure S26. ^{119}Sn NMR spectrum of **2-SnP** in $CDCl_3$

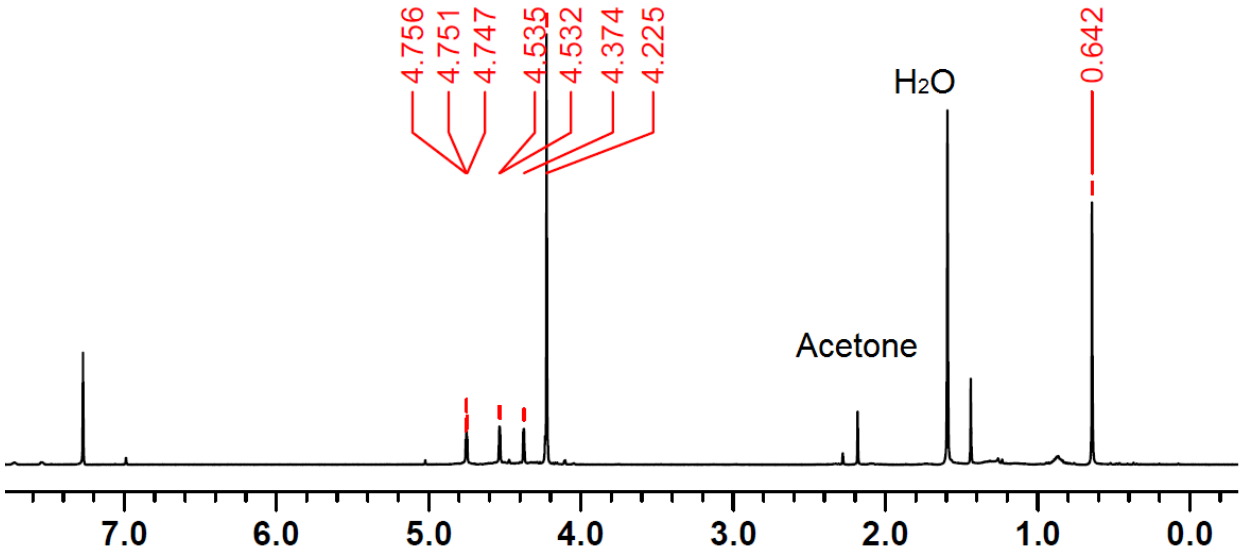

Figure S27. ^{1}H NMR spectrum of intermediate **$Fc_2SiMe_2Hg_2Cl_2$** in $CDCl_3$

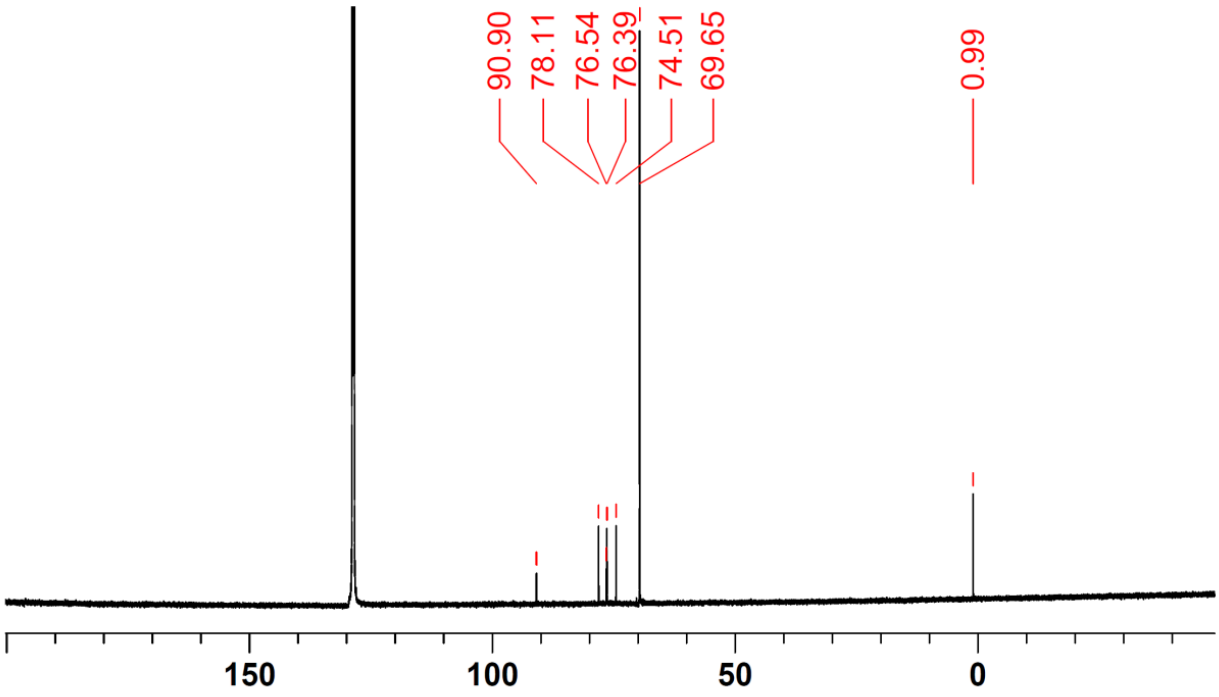

Figure S28. ^{13}C NMR spectrum of intermediate **$Fc_2SiMe_2Hg_2Cl_2$** in C_6D_6

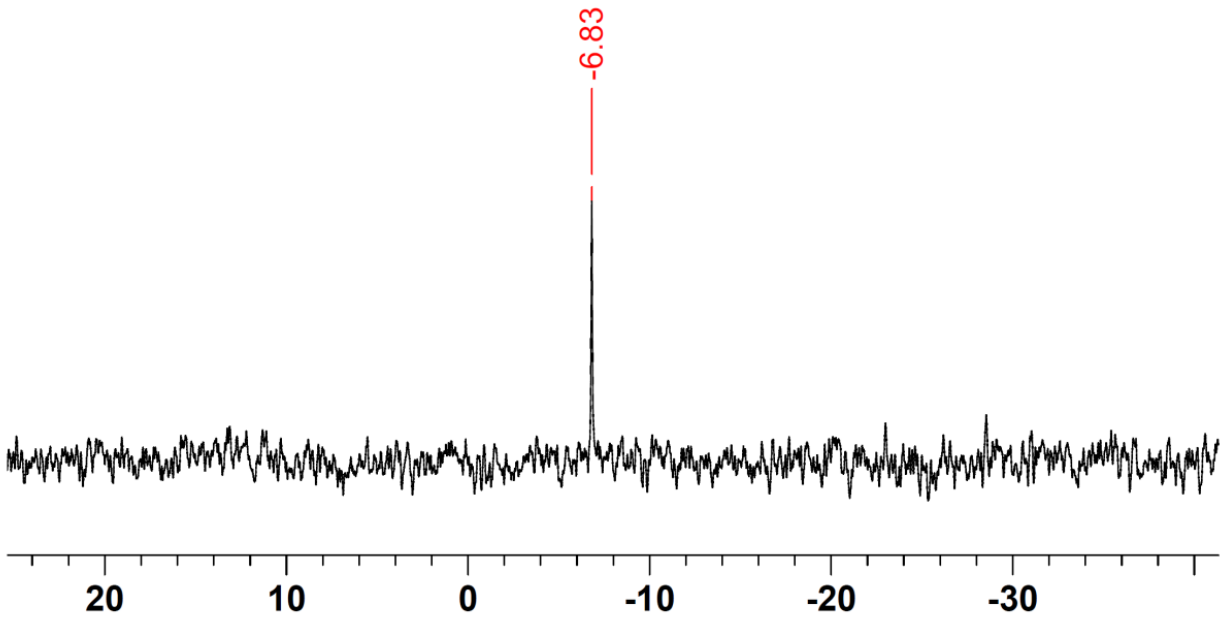

Figure S29. ^{29}Si NMR spectrum of intermediate **$Fc_2SiMe_2Hg_2Cl_2$** in C_6D_6

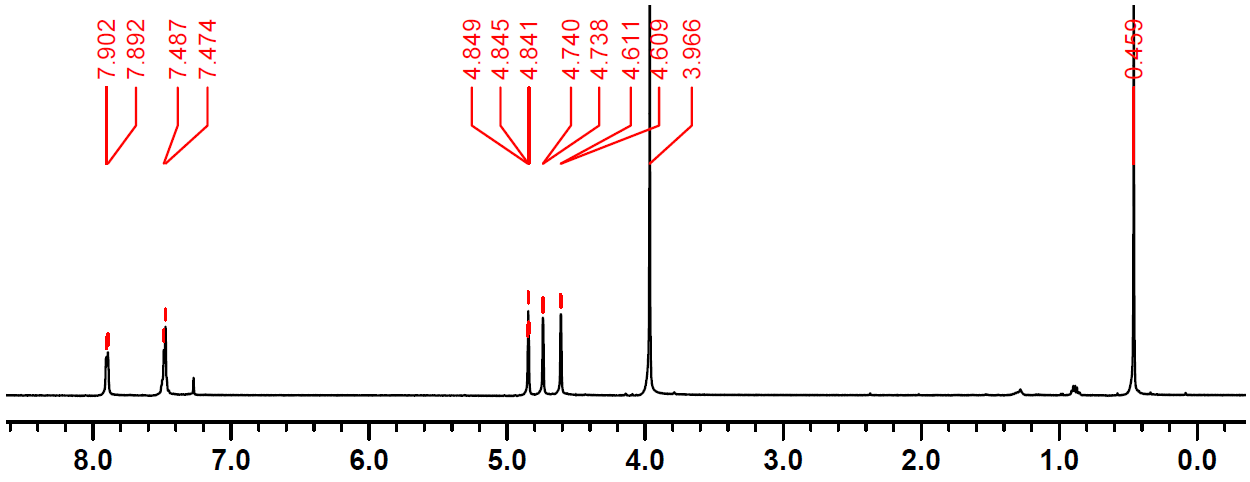

Figure S30. ^{1}H NMR spectrum of **2-BSi** in $CDCl_3$

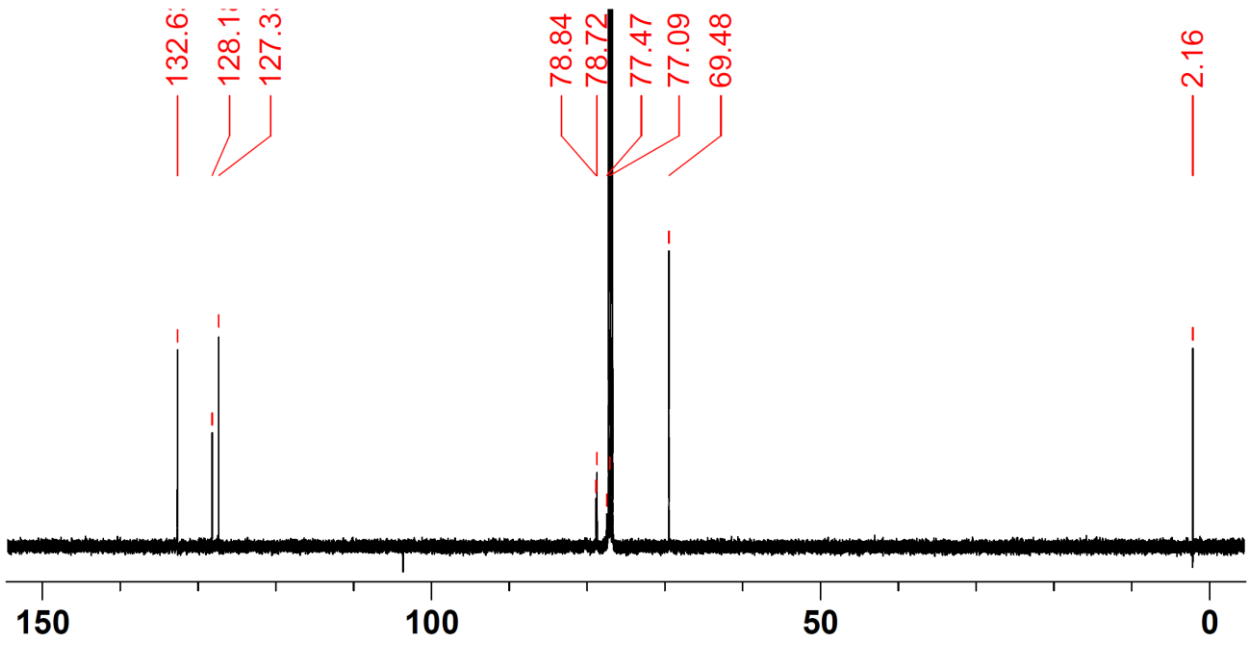

Figure S31. ^{13}C NMR spectrum of **2-BSi** in $CDCl_3$

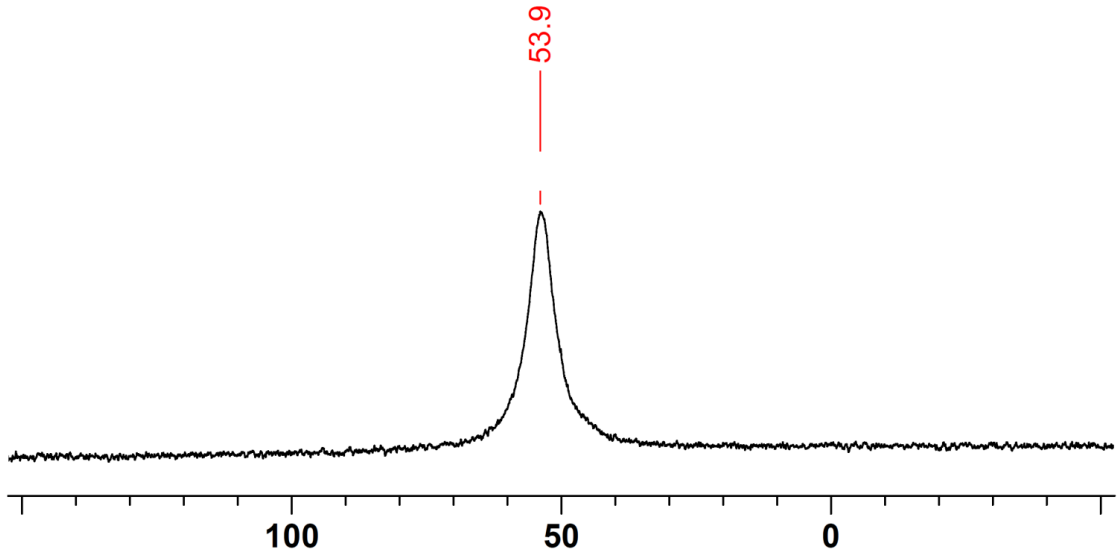

Figure S32. ^{11}B NMR spectrum of **2-BSi** in $CDCl_3$

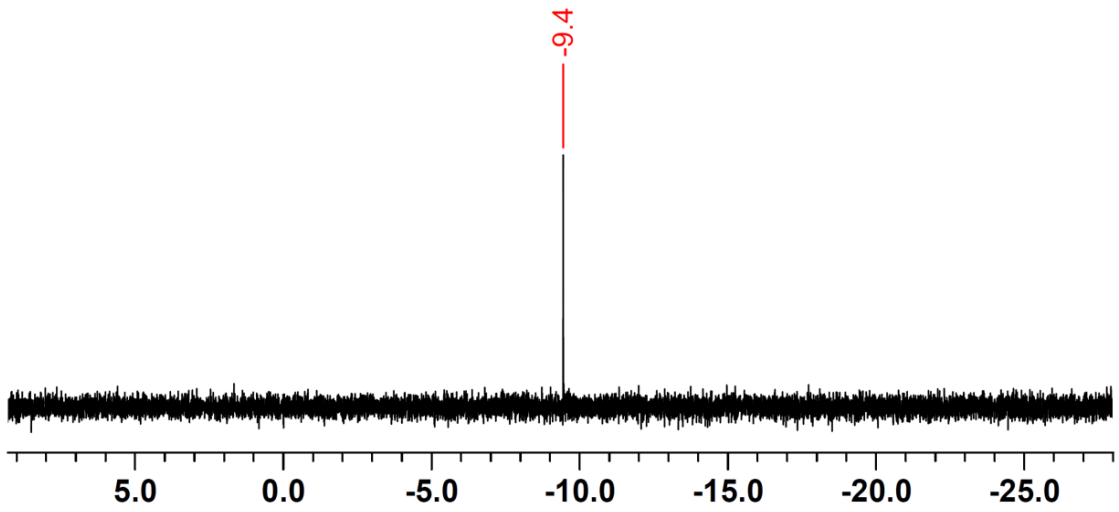

Figure S33. ^{29}Si NMR spectrum of **2-BSi** in $CDCl_3$

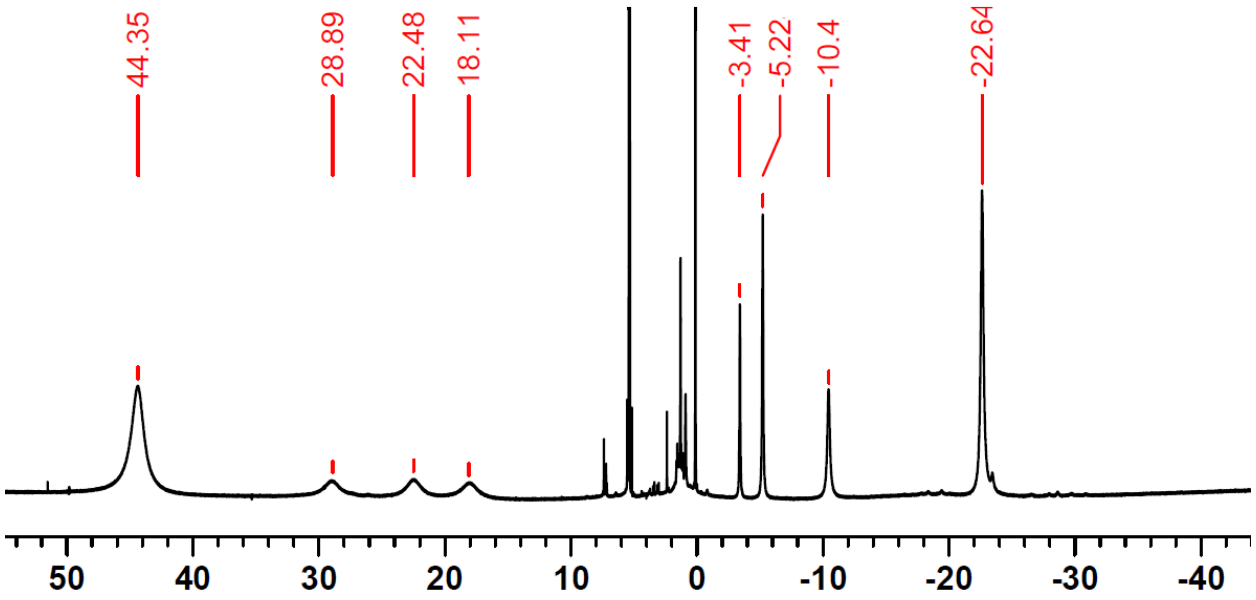

Figure S34. ^{1}H NMR spectrum of doubly oxidized **2-BSi** in CD_2Cl_2

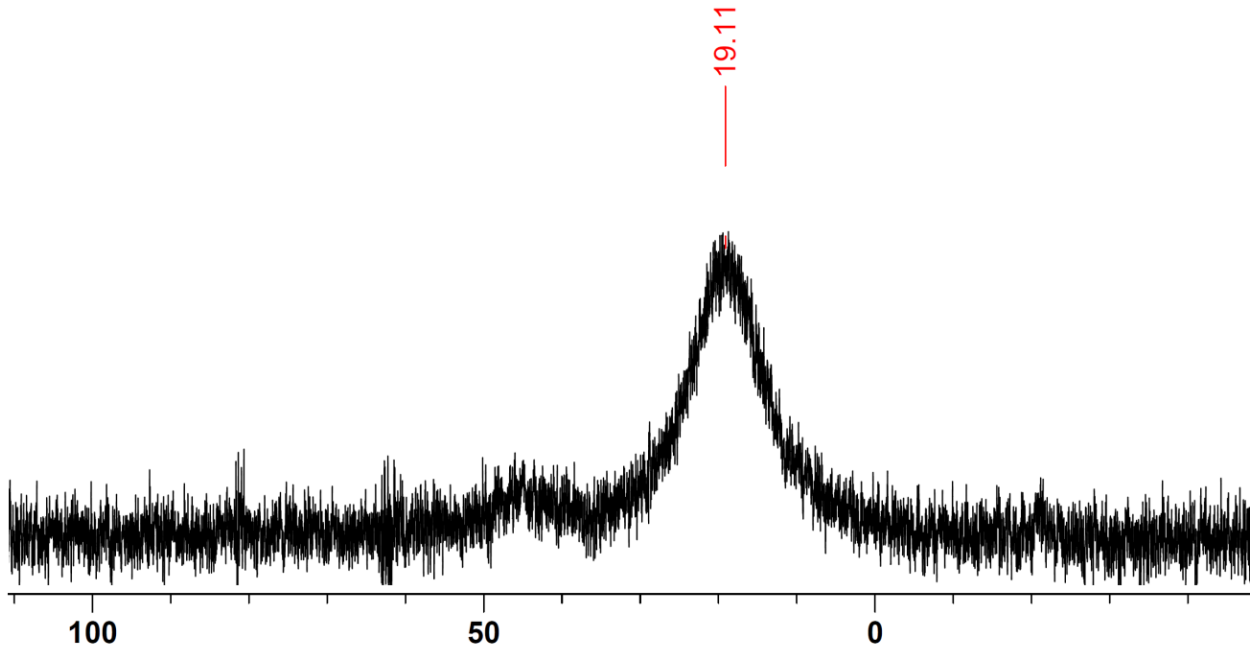

Figure S35. ^{11}B NMR spectrum of doubly oxidized **2-BSi** in CD_2Cl_2

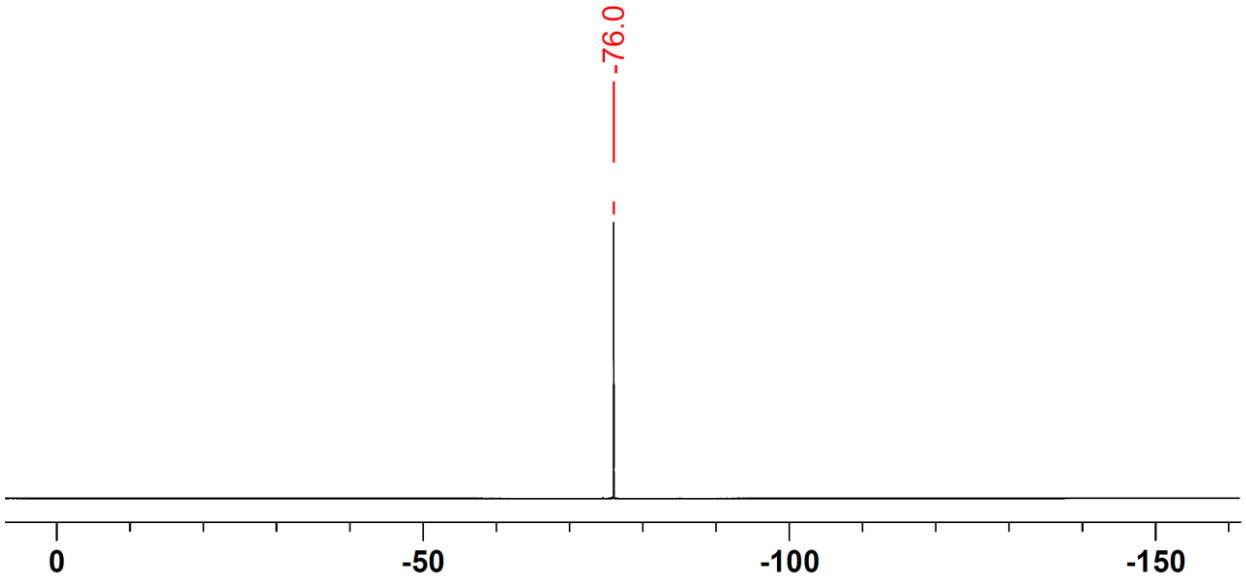

Figure S36. ^{19}F NMR spectrum of doubly oxidized **2-BSi** in CD_2Cl_2

COPIES OF HIGH-RES MASS SPECTRA

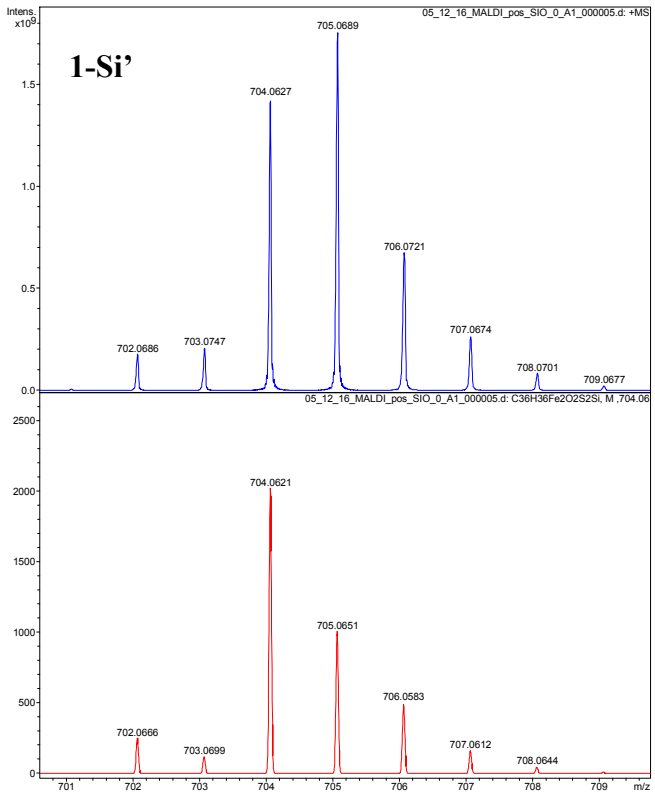

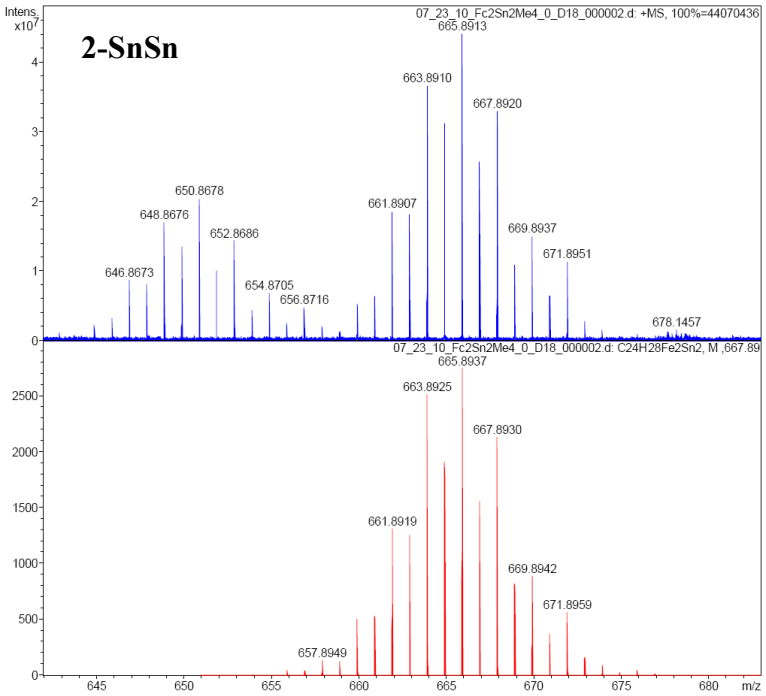

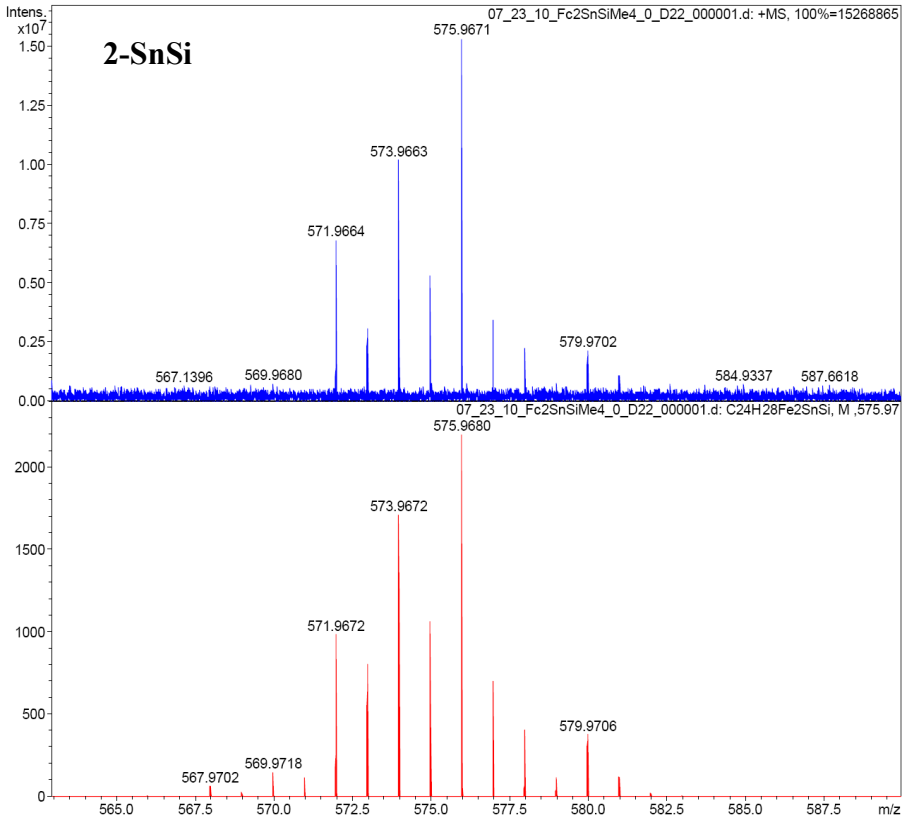
2-SnSi
Intens.
x10^7
07_23_10_Fc2SnSiMe4_0_D22_000001.d: +MS, 100%=15268865
575.9671
573.9663
571.9664
579.9702
567.1396
569.9680
584.9337
587.6618
07_23_10_Fc2SnSiMe4_0_D22_000001.d: C24H28Fe2SnSi, M ,575.97
575.9680
573.9672
571.9672
579.9706
569.9718
567.9702
m/z

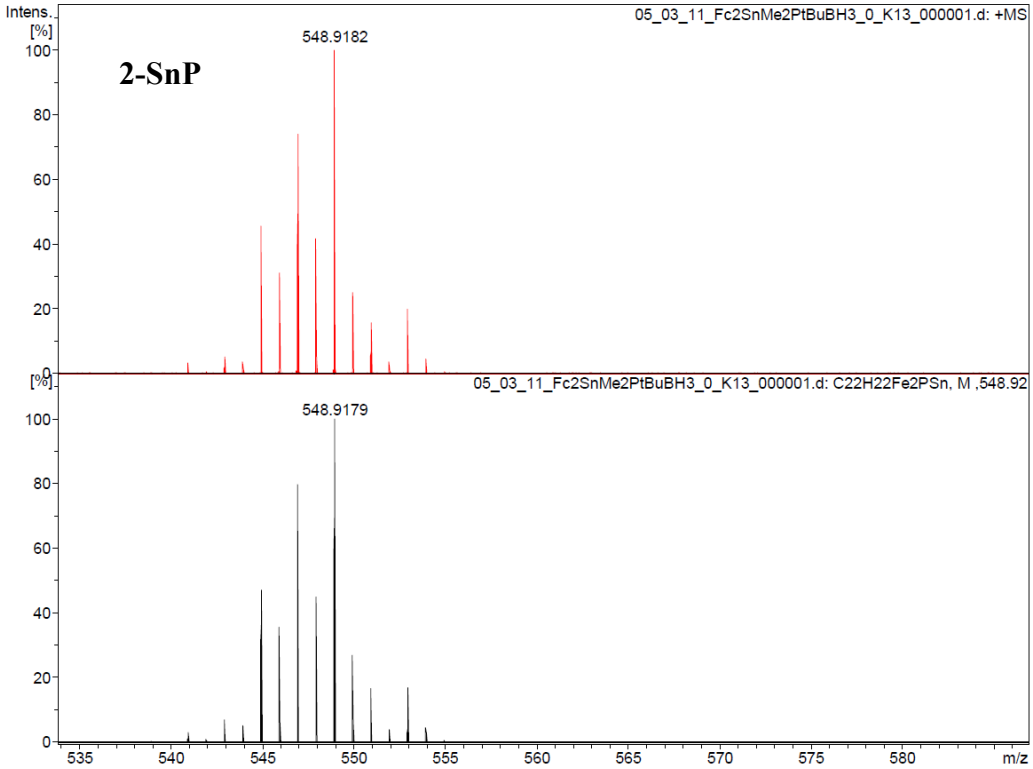
2-SnP
Intens.
[%]
05_03_11_Fc2SnMe2PtBuBH3_0_K13_000001.d: +MS
548.9182
05_03_11_Fc2SnMe2PtBuBH3_0_K13_000001.d: C22H22Fe2PSn, M ,548.92
548.9179
m/z

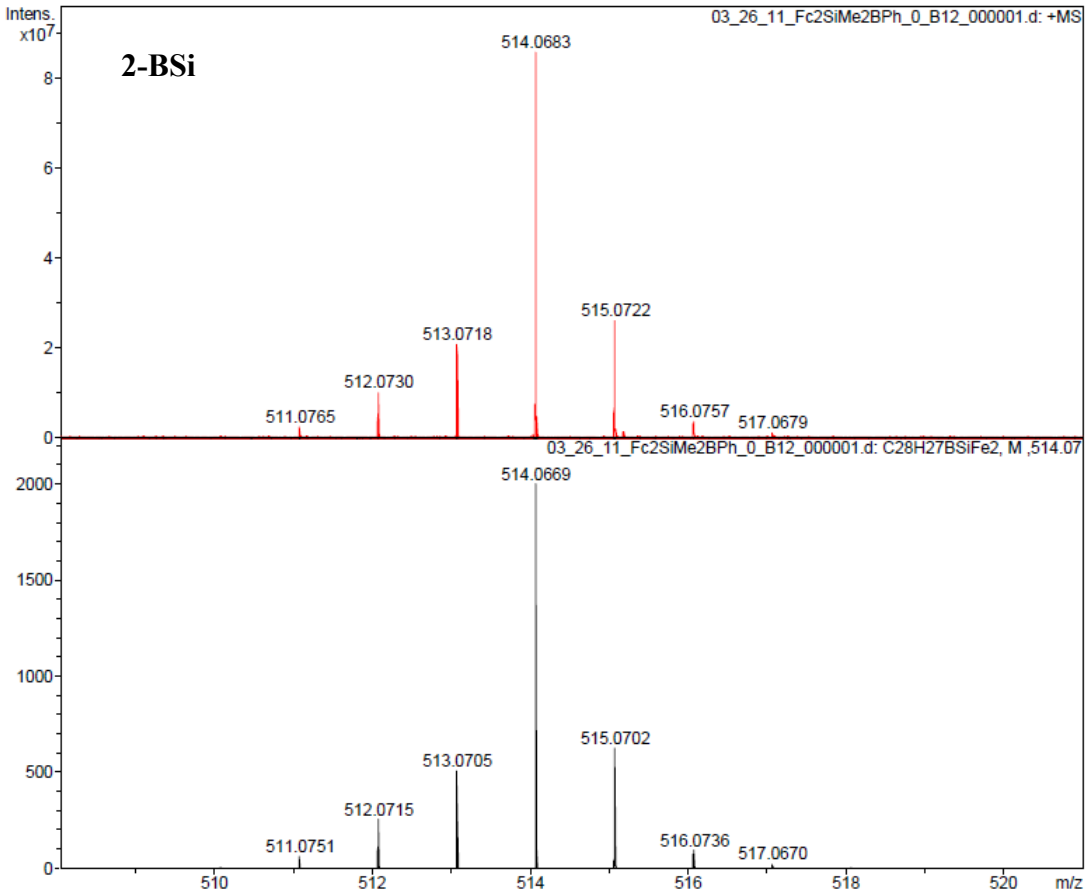

Figure S37. MALDI-MS data of compounds **1-Si'**, **2-SnSn**, **2-SnSi**, **2-SnP** and **2-BSi**